Sustainable Production and Consumption 32 (2022) 519–531

Contents lists available at ScienceDirect

Sustainable Production and Consumption

journal homepage: www.elsevier.com/locate/spc

Research article

Pyrolysis of all layers of surgical mask waste as a mixture and its life-cycle assessment

Samy Yousef [a,*], Justas Eimontas [b], Inga Stasiulaitiene [c], Kęstutis Zakarauskas [b], Nerijus Striūgas [b]

[a] Department of Production Engineering, Faculty of Mechanical Engineering and Design, Kaunas University of Technology, LT-51424 Kaunas, Lithuania
[b] Lithuanian Energy Institute, Laboratory of Combustion Processes, Breslaujos 3, LT-44403 Kaunas, Lithuania
[c] Department of Environmental Technology, Faculty of Chemical Technology, Kaunas University of Technology, LT-50254 Kaunas, Lithuania

ARTICLE INFO

Article history:
Received 3 March 2022
Received in revised form 7 May 2022
Accepted 8 May 2022
Available online 16 May 2022

Editor: Prof. Carmen Teodosiu

Keywords:
Surgical mask waste
Pyrolysis
Pyrolysis oil
Wax
Gaseous
Life cycle assessment

ABSTRACT

Most of the waste generated from surgical masks waste (WMs) consists of three layers made of conventional nonwoven fabric (upper and lower layers) and a molten blown polypropylene filter mixed with other polymeric additives (middle layer). All these layers are held together by a friction bonding, hence making their separation a difficult task. Their recycling as a mixture is the most cost-efficient solution without the need for further treatments. Within this framework, this research aims to study the pyrolysis of all layers of WMs as a mixture using an experimental set-up with capacity of 200 g at different pyrolysis temperatures (475, 500, 525, and 550 °C). The distributions of gases formulated during the entire process were observed. Also, the composition of the obtained pyrolysis products was examined. Finally, the environmental impacts of the proposed process and its environmental benefits were studied using life cycle analysis (LCA-Simapro) based on two different scenarios (oil and wax production). The results showed that at 500 °C, the highest oil yield was achieved (42.3%) and smaller amounts of gaseous (54.1%) and calcium-rich char (3.6%) products were generated, while other samples produced wax product with lower yield in the range of 21–36%. The gases measurements showed that methane, ethane and propane were the major gases in the gaseous products, while carbon dioxide and carbon monoxide gases were completely absent. Meanwhile, the GC/MS results showed that the obtained gaseous, oil, and wax products were very rich in flammable compounds, especially 2,4-Dimethyl-1-heptene compound with abundance of 33–38% (gaseous) and 12.5–23.8% (tars). Finally, the LCA results showed that the management of WMs as a mixture via pyrolysis significantly reduced the Global warming potential factor up to 0.244 kg CO_2 eq/kg (oil) and 0.151 CO_2 eq/kg (wax) with improvement by 90–94%, when compared to incineration management. However, the economic analysis showed that the oil production scenario has a significant contribution to the economic sector with an 85% improvement.

1. Introduction

Currently, more than 129 million surgical mask waste (WMs) are produced every monthly due to their short life and single use (Lee et al., 2021a, 2021b, 2021c). This type of waste represents a major fraction of medical waste and contains many plastic materials in the form of fibres (Sangkham, 2020). These WMs generally consist of three layers distributed in the vertical direction as follows: traditional two nonwoven fabrics (upper and lower layers) and middle layer (molten blown filter) made of polypropylene as a base polymeric material mixed with other polymer fillers (e.g., Polyethylene terephthalate, Polyamide, Polyethylene, Polyurethane, etc.) (Forouzandeh et al., 2021; https://blog.gotopac.com; Tcharkhtchi et al., 2021). All these layers are joined by a mechanical bond resulting from the friction between polymeric fibres [https://www.fda.gov]. These WMs are classified as non-biodegradable waste and have a negative impact on the environment and human health (Torres and De-la-Torre, 2021). Besides, it is a new source for producing microplastics that have several serious consequences on living organisms and marine life (Ray et al., 2022; Liang et al., 2022). Despite all these misfortunes, these masks

Abbreviations: WMs, Surgical masks waste; H_2, Hydrogen; CO, Carbon monoxide; CO_2, Carbon dioxide; CH_4, Methane; C_2H_4, Ethylene; C_2H_6, Ethane; C_3H_8, Propane; FTIR, Fourier Transform Infrared spectroscopy; GC–MS, Gas chromatography-mass spectrometry; SEM-EDX, Scanning electron microscopy; EDX, Energy dispersive X-Ray analysis; LCA, Life cycle analysis; TGA, thermogravimetric analysis; DTG, Derivative thermogravimetric; N_2, nitrogen; Ca, calcium; SR, solid residues; $CaCO_3$, Calcium carbonate; GW, Global warming; OFH, Ozone formation, Human health; FP, Fine particulate matter formation; OFT, Ozone formation, Terrestrial ecosystems; TA, Terrestrial acidification; TE, Terrestrial ecotoxicity; FR, Fossil resource scarcity.

* Corresponding author.
E-mail address: ahmed.saed@ktu.lt (S. Yousef).

https://doi.org/10.1016/j.spc.2022.05.011
2352-5509/

can decompose under the influence of thermal treatment (e.g., pyrolysis, gasification, carbonization, etc.) into hydrocarbon compounds, gases rich in hydrogen with high heating values and economic benefits, and hybrids nanoparticles (Carbon nanotubes/Nickel). (Dharmaraj et al., 2021; Farooq et al., 2022; Yu et al., 2021). In addition, these practical uses help to reduce emission of nitrogen oxides from incineration process (Lan et al., 2022). Among the various thermal practices, pyrolysis treatment is one of the most promising solutions for valorisation of the millions of WMs (individually or mixed with motor oil and biomass) produced monthly around the world and converting them into energy products (flammable liquid, gaseous, volatile organic compounds, and carbon black) with higher heating value compared to other processes (Purnomo et al., 2021; Ardila-Suárez et al., 2022).

Several studies have been carried out to anchor this principle in various laboratory-wide research criteria. Some of the research were carried out to study thermal decomposition of WMs using thermogravimetric analysis (TGA) under different heating conditions (Sun et al., 2021). The results showed that the masks decompose into three regions, and the primary decomposition region is in the range 400–500 °C with an estimated weight loss of 95 wt% (Brillard et al., 2021). Based on TGA measurements, the pyrolysis kinetic of WMs and its decomposition mechanism was studied using differential isoconversional method as a one of the most accurate methods in calculating the kinetic parameters of materials, which is complicated as it tends to take place in multiple steps with different reaction rates. The results showed that the average activation energies were in the range of 158–281 kJ/mol (Eimontas et al., 2021a). Also, the experimental derivative thermogravimetric (DTG) curves were also modelled using several methods and their model parameters were estimated. Meanwhile, volatile compounds in the formulated pyrolysis vapours in the core decomposition region were detected using Fourier Transform Infrared (FTIR) spectroscopy, which showed that the WMs are very rich in aromatic and aliphatic compounds, especially at higher heating rates >20 °C/min. Furthermore, the compositions of these groups were analysed again using gas chromatography–mass spectrometry (GC–MS) and the effect of heating temperature on them was assessed (Eimontas et al., 2021b; Jung et al., 2021). The GC–MS results showed that 2,4-Dimethyl-1-Heptene is the main compound in the volatile products with abundance >43%. In order to increase the productivity of the aromatic compounds and volatile products in the pyrolysis products, various zeolite catalysts (e.g., HZSM-5, HBeta, ZSM-5, HY, ZSM-5, etc.) were used during the conversion process (Lee et al., 2021a, 2021b, 2021c; Ali et al., 2022; Yousef et al., 2022).

Despite these promising results, this type of measurements and analyses gives only the basic results of the decomposition process and cannot be used to determine its environmental impact of the entire process, which depends on the inputs, outputs, and emissions of the components (Shammi et al., 2022). The study of the environmental impact is critical for clarification of technological emissions as a whole and for each process and it may help to improve its performance (Lee et al., 2021a, 2021b, 2021c). Within this framework and to provide more information on environmental performance and encourage investors to spend on such emerging technologies, Chao et al. (2021) studied the pyrolysis of WMs a fixed-bed reactor (up to 650 °C) and its life-cycle assessment (LCA) (Li et al., 2022a, 2022b, 2022c). Although the study succeeded in providing some preliminary information about the yield, the optimum pyrolysis temperature (500 °C) and LCA of entire process, however, the experiments were performed on each WMs layer separately (lower, middle, and upper layer), hence, needing additional sorting and pre-treatment processes to separate WMs layers (Gala et al., 2020; Mumladze et al., 2018). Unfortunately, these processes were neglected in the suggested LCA, what affected credibility of LCA results and sequence of operations. Therefore, treatment of all layers of WMs as a mixture is the closest approach to industrial reality and allows avoiding additional treatments and putting workers at risk of infection, especially as some of these WMs are loaded with viruses (Amuah et al., 2022; Kang et al., 2021). Within this context, this research aims to investigate the pyrolysis of all layers of WMs as a mixture (lower, middle, and upper) and its LCA using an experimental set-up with capacity of 200 g at different pyrolysis temperatures in the range 475–550 °C. Also, the effect of pyrolysis temperature on the composition of the generated tar, gaseous, char products was examined using GC–MS and scanning electron microscopy (SEM) with energy dispersive X-Ray analysis (EDX). Finally, LCA was studied for all the proposed processes under optimal pyrolysis conditions necessary to produce oil (scenario A) and wax (scenario B).

2. Experimental

2.1. Materials and WMs feedstock preparation

The WMs in series of 3-ply face masks (consisting of traditional two nonwoven fabrics and single molten blown filter layer) were used as a feedstock in the present study because of them belonging to the most commercial type that costs less and manifests good hypoallergenic and breathing resistance performances (Das et al., 2021). Besides, this kind of waste is very rich in carbon (84.7%) and volatile matter (96.6%) (Eimontas et al., 2021). The specified masks were collected and sorted from the local hospital in Lithuania followed by cutting the fabric layers (without ropes) into small pieces, then grinding them into fine particles using an electrical grinder to prepare them for the pyrolysis experiments. The pre-treatment usually has the purpose to reduce size and to increase contact between the surfaces and the heat flux, thus helping heat to exchange and leading to faster decomposition using different thermochemical treatment (Striūgas et al., 2021; Abdelnaby et al., 2021).

2.2. Pyrolysis experiments

The pyrolysis of WMs was performed in an experimental set-up in nitrogen (N_2) at a flow rate of 60 mL/min. The set-up contained a thermochemical reactor, a gas purification and cooling unit, and a primary gas detection unit. In addition, there were two different depots for collecting of the obtained products (tars and the condensate volatiles components), while the char remained on the bottom of the decomposition chamber. The experiments were started by placing the sample (200 g) into the reactor's inlet (unheated), then removing oxygen from the reaction chamber by purging it with N_2 for 10 min before each run (Zakarauskas et al., 2021); then the main decomposition process would start at a constant heating rate of 25 °C/min and four different pyrolysis temperatures: 475, 500, 525, and 550 °C. These conditions were selected based on the main decomposition regions, which were received from thermogravimetric results in our previous study. Based on TG-FTIR and GC–MS results, the highest amount of volatile, aromatic, and aliphatic compounds can be achieved at 25 °C/min (Eimontas et al., 2021a); therefore, 25 °C/min was selected as an optimum heating rate in the present work. When the reactor reached the specified temperature, the feedstock was pushed into filtered capsule to initiate pyrolysis experiments. The formulated tar products (oil and wax) were collected into an empty tank fixed at the bottom of the reactor. Other light volatiles products mixed with gases were condensed in four condensers distributed in series and filled with 75 ml of propanol per unit to continue absorbing the condensable volatile products (Mohamed et al., 2021). All these condensers were combined in a container with salt water for cooling. At the rear of the plant, Tedlar gas bag was used to collect the generated gaseous products. Meanwhile, the online measurement unit was used to check the concentration of O_2, CO_2, CO, H_2, and CH_4 in the gaseous products during the entire process. All components and construction of the used plant are illustrated in Fig. 1. By the end of the experiments, the reactor's heating was stopped immediately, and cooling to room temperature would start followed by chamber opening and solid powder product (char) extraction, then

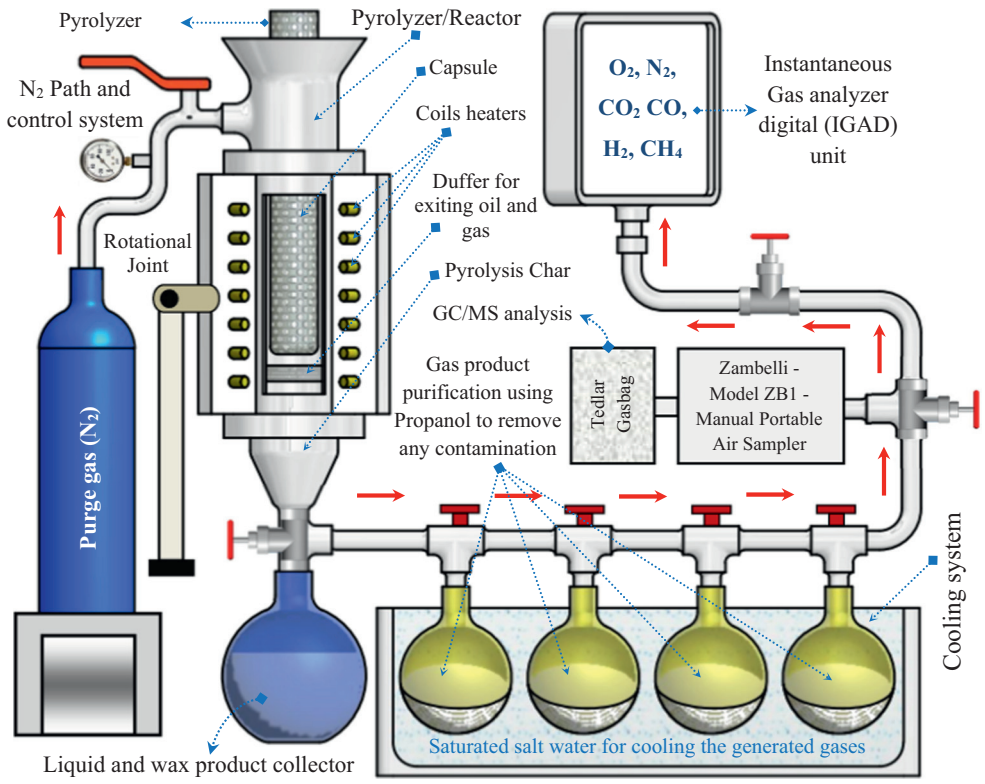

Fig. 1. The complete design of the pyrolysis plant used in the conversion process.

weighing and calculating its yield, while the yield of oil product was calculated, and the gas product yield was determined by subtracting the solid residue and oil or wax yields (Trofimov et al., 2020).

2.3. Characterizations of the pyrolysis products

The tars, gaseous, char components produced by the end of pyrolysis treatment at various temperatures (475, 500, 525, 550 °C) were analysed using FTIR and GC–MS (Shimadzu GC-2010). The chemical structure and crystal structure of the obtained char were examined using FTIR. Besides, the morphology and chemical composition of char fraction were observed using SEM-EDX (Model BPI-T).

2.4. Environmental impact from the life cycle's perspective

LCA was used in the present study to assess environmental impacts and other impact factors on the whole WMs products and their treatment using catalytic pyrolysis process. The assessment was performed according to the recommendations and Guidelines of international environmental standards (ISO, 2006), by defining the following items: goal and scope definition, inventory data collection, and impact assessment with explanation (Santos et al., 2022).

2.4.1. Definition of the goal and scope

The LCA aimed to estimate the potential environmental impacts of oil recovery (scenario A) and wax recovery (scenario A) from pyrolysis

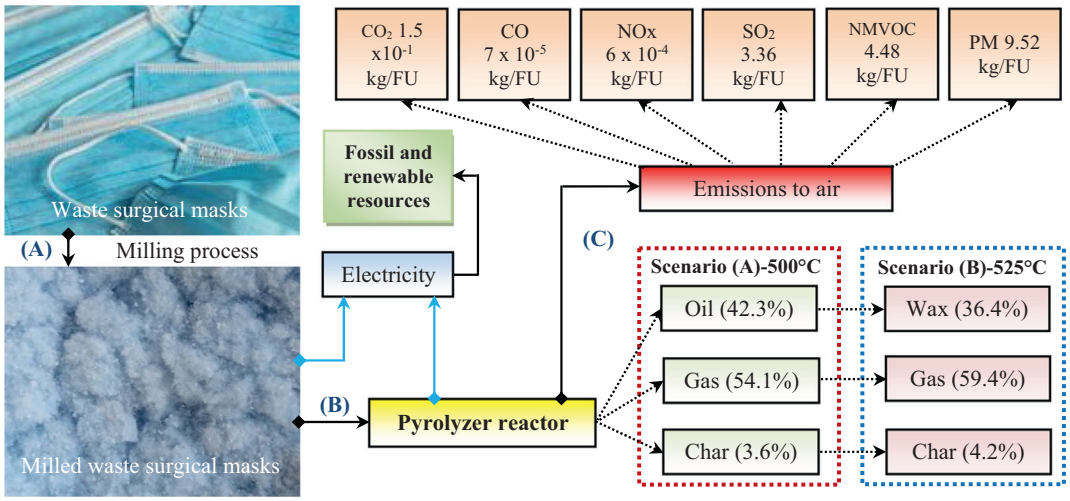

Fig. 2. The layout of the experiments and analysis' flowchart.

of WMs. The results were compared with traditional disposal practices, in particular incineration of polypropylene (main component in WMs) to determine the technical and ecological potentials of the suggested treatment. The functional unit was defined as 1 kg of WMs, and the geographical background was set in the European region, while the hypothetical scenarios for the use of the developed system are shown in Fig. 2. As shown, the transportation facility was neglected in LCA and the system boundary covers two phases: pre-treatment by shredding to reduce WMs size, followed by conversion of WMs into oil and wax products.

Since tar products (oil and wax) represent the most profitable pyrolysis products, the suggested scenarios (A, B) were designed based on the present experimental results, which achieve maximum yield of tar: oil (42.26%) at 500 °C and wax (36.44%) at 525 °C, as shown in the results' section. It was assumed that the energy inputs in both scenarios were accumulated from shredding and pyrolysis plant. Finally, the LCA was carried out using the ReCiPe midpoint approach to estimate the most frequent impact categories, which were used to investigate the energy and waste treatment methods (Dastjerdi et al., 2021; Mayanti and Helo, 2022).

2.4.2. Collection of inventory data

This section was dedicated to collect the required input and output data for the suggested layout. The cost of collecting WMs has been neglected because unfortunately until now there is no clear industrial vision for the collection of masks which makes the estimation of the costs of collection and sorting an inaccurate estimate and further studies are needed for that purpose. The consumed energy required for pre-milling procedure of WMs and its conversion into short fibres with lower crystallinity helps to accelerate the conversion process (Yousef et al., 2021; Kuliešienė et al., 2021), which was estimated at 0.011 kWh/kg since WMs have a very soft fabric structure (Naimi and Sokhansanj, 2018), and this value was assumed as an input energy for the proposed layout of pre-treatment. The consumed energy during the main thermal conversion treatment using pyrolysis at 500 °C was calculated in the laboratory and estimated from our previously published work as 1.25×10^{-01} kWh/kg (Kliucininkas et al., 2019a, 2019b). The emission data from the pyrolysis process of WMs was collected from the literature on polypropylene plastic waste (Khoo, 2019). Regarding the outputs, three different products (oil or wax, gas, and char) were received from the two selected samples (500 and 525 °C) and all the inventory data extracted from the literature and Ecoinvent 3.7 database model (in LCA program) are summarized in Table 1. The heating values of the oil, waxes, gaseous, and char products reported in the literature are 24 MJ/kg, 45 MJ/kg, 6.7 MJ/kg, and 28 MJ/kg, respectively (https://pyrotechenergy.com/; Abdy et al., 2022a, 2022b) they were recalculated again based on the yield of each product listed in Table 2.

Table 1
Inventory data of pyrolysis of function unit of WMs.

Parameter	Definition	500 °C (Oil)	525 °C (Wax)
Input	Electricity for pre-treatment	0.011 kWh/kg	
	Electricity for pyrolysis	1.25×10^{-01} kWh/kg	
Outputs	Pyrolysis oil or wax	10.14 MJ/kg	16.4 MJ/kg
	By-products-Char	1 MJ/kg	1.2 MJ/kg
	By-products-Gaseous product	3.6 MJ/kg	3.97 MJ/kg
Emissions to air	CO_2	1.50×10^{-01} kg/FU	
	CO	7.00×10^{-05} kg/FU	
	NO_x	6.00×10^{-04} kg/FU	
	SO_2	$3.36 \times 10^{+00}$ kg/FU	
	NMVOC	$4.48 \times 10^{+00}$ kg/FU	
	PM (dust)	$9.52 \times 10^{+00}$ kg/FU	

Table 2
Yields of the pyrolyzed WMs at different pyrolysis temperatures.

Pyrolysis product	Yield of each sample referred to pyrolysis temperatures			
	475 °C	500 °C	525 °C	550 °C
Oil (wt%)	–	42.26	–	–
Wax (wt%)	21.42	–	36.44	34.67
Gas (wt%)	72.00	54.13	59.38	60.81
Char (wt%)	6.58	3.61	4.18	4.52

3. Results and discussion

3.1. Yields and distribution of pyrolysis products

Once the pyrolysis treatment of masks had been finished, the yields of oil/wax, gaseous, and solid residue products at the specified pyrolysis temperatures (475, 500, 525, and 550 °C) were calculated based on the weight balance and the results are summarized in Table 2. As shown, the pyrolysis temperature has a significant impact on the yield, distribution, and composition of the formulated pyrolysis products, where at 475, 525, and 550 °C, wax was the main tar product with estimated yield of 21.42, 36.44, and 34.67%, respectively, and the yield of char and gaseous products was in the range of 4.2–6.6% and 59.4–72%, respectively. Meanwhile, at 500 °C pyrolysis temperature, the biggest amount of liquid tar (42.3%) and the smallest amount of gas (54.1%) and char (3.6%) were obtained. As shown, at lower pyrolysis temperature (475 °C), the gaseous product was the predominant product with the largest amount of char and a small amount of wax. At 500 °C, the cracking reaction was promoted to convert wax fraction into oil with minimal number of gaseous and char products, while higher pyrolysis temperatures (525 and 550 °C) led to promotion of the cracking reaction and evaporation of the liquid part from oil and its conversion into gas under the applied temperature, where the yield of gaseous product increased at the expense of oil.

Since the ideal conversion process using pyrolysis treatment occurs in nitrogen ambient without any O_2, the distribution of these gases was observed during the entire process using IGAD unit and the results are shown in Fig. 3. It seems that the treatment was conducted in nitrogen atmosphere without any O_2 gas, hence proving that the process was performed according to the standard conditions (Li et al., 2022a, 2022b, 2022c). The distributions of H_2, CO, CO_2, CH_4, and C_2H_4 gases in the formulated gaseous products at different pyrolysis temperatures showed that CH_4 was the major compound in all samples and its abundance increased as temperature was increasing up to 77%. Meanwhile, no presence of other gases (H_2, CO, CO_2, and C_2H_4) was noticed. However, these measurements are sometimes deceptive because such measurement methods are applied with methane cell (Eimontas et al., 2021; Šereika et al., 2021), which is used to check C—H groups only and presence of other light hydrocarbon compounds, such as C_2H_6 and C_3H_8, so, the device treats all gases as CH_4 compound. Usually, GC analysis is used to eliminate this confusion and to get correct chemical compositions. Based on that, GC was used to analyse these compounds again in the next section.

3.2. GC analysis of gaseous products

During the conversion process of WMs in pyrolysis plant, six samples of gaseous products were stored in Tedlar gasbags at different degradation temperatures in the range of 450–550 °C. This range was determined based on the major decomposition regions which were established using TGA in our previous study (Eimontas et al., 2021). The gaseous products collected using a portable constant flow sampler at the specified conditions were analysed using GC–MS and the gases distributions are summarized in Fig. 4A-D without considering O_2 and N_2 gases. As shown, CH_4, C_2H_6 and C_3H_8 were the major compounds in all batches with different abundances along with a weak presence of H_2

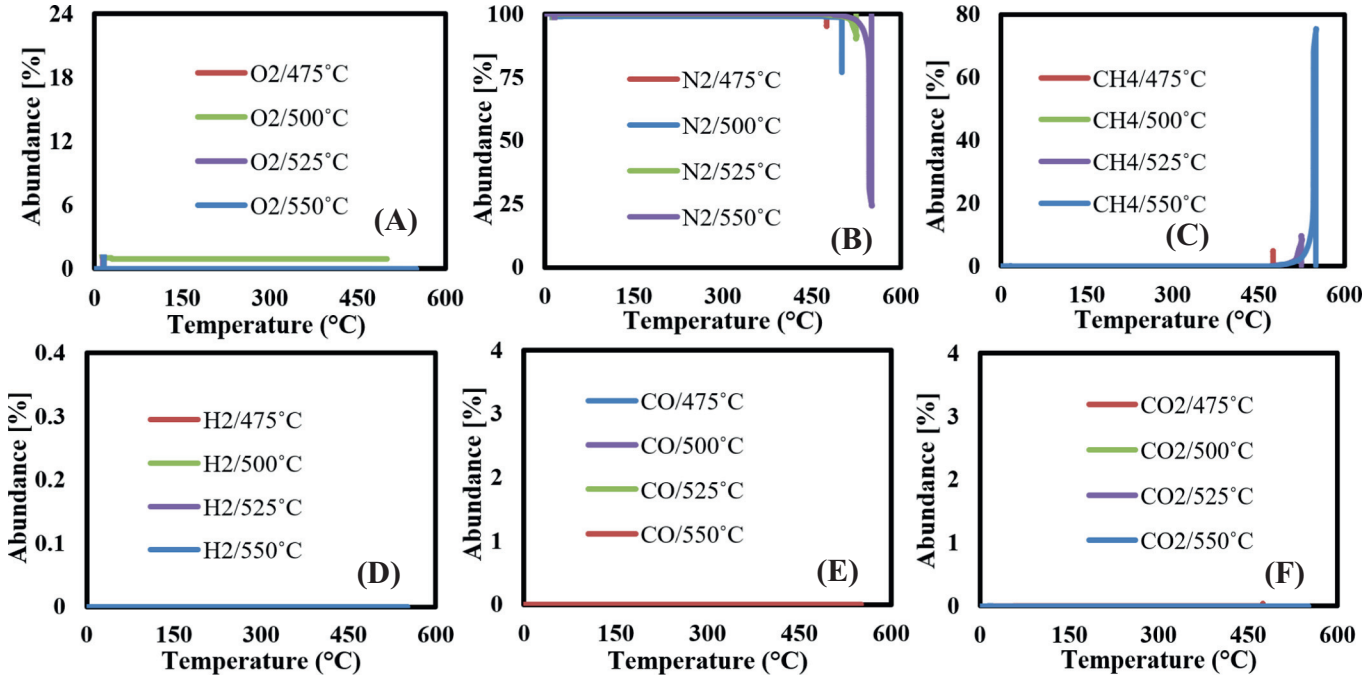

Fig. 3. Distributions of A) O_2, B) N_2, C) CO_2, D) CO, E) CH_4, and F) H_2 gas in the gaseous products during the entire conversion process.

observed in the 550 °C sample due to cracking of aliphatic structures and their chains (Papari et al., 2021). Also, it was noticed that the gaseous products synthesized from samples that were pyrolyzed up to 500 °C and 550 °C appeared to be completely CO_2-free and C_2H_6 and C_3H_8 were the major gases in these batches. As the treatment time increased up to 55 and 60 min, C_3H_8 became the main compound of the formulated gaseous product, where higher conditions allowed stronger cracking reaction and formation of more of CH_4 compound (Li et al., 2022a, 2022b, 2022c). As temperature increased more, CH_4 compound started to participate in the cracking reaction to generate

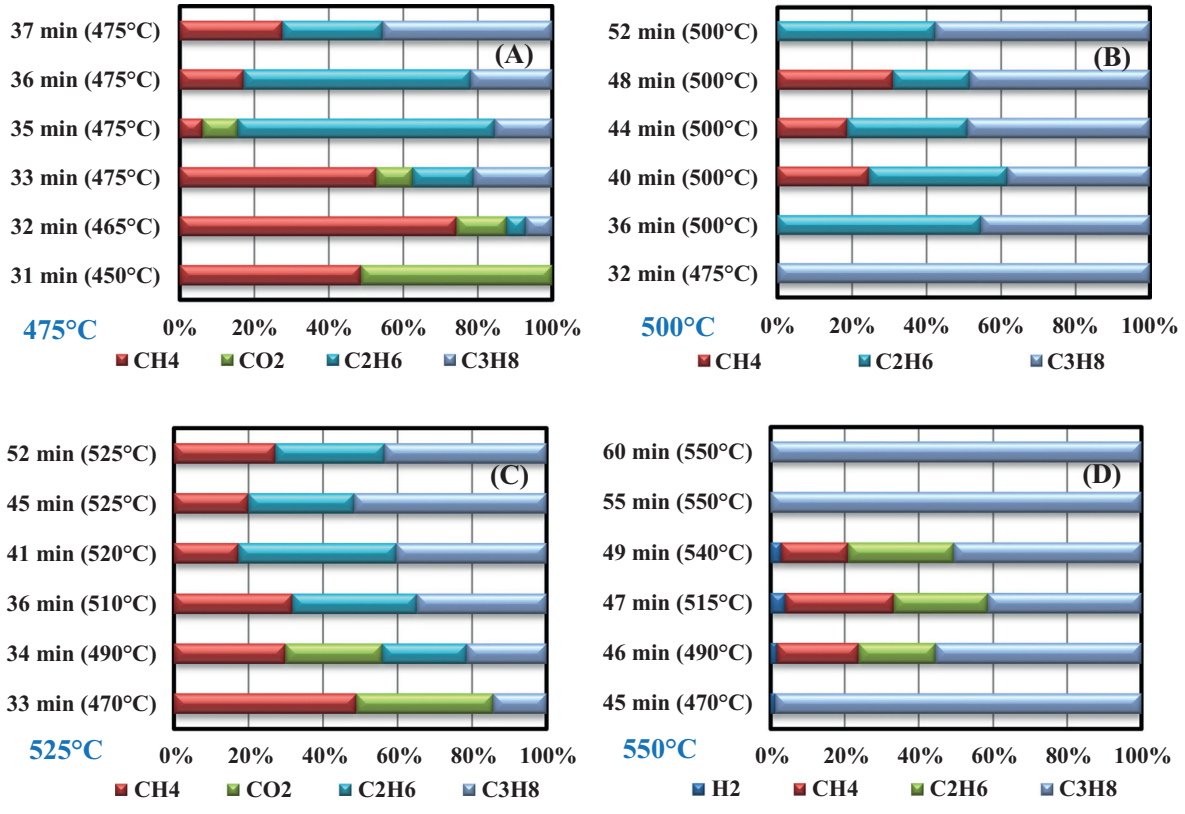

Fig. 4. GC analysis of the gaseous products synthesized from the pyrolyzed WMs samples at A) 475 °C, B) 500 °C, C)500 °C and D) 550 °C at different decomposition temperatures.

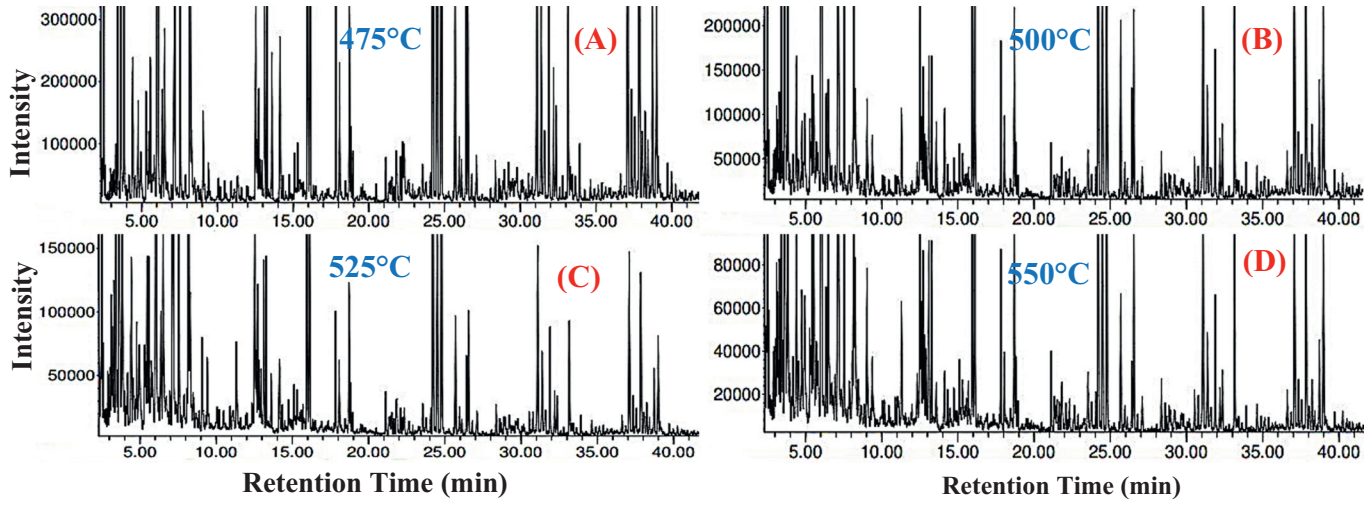

Fig. 5. GC/MS of the obtained gaseous products at A) 475 °C, B) 500 °C, C)525 °C and D) 550 °C.

more C_2H_6 and C_3H_8 compounds after integrating their radicals (Praspaliauskas et al., 2020). Also, some quantities of CO_2 were observed at lower temperatures due to the decarboxylation reaction and ester groups in the feedstock. Longer treatment time led to decomposition of the formed CO_2 into gases (Xu et al., 2022). Although the gaseous products received from 475 °C and 525 °C samples were rich in CH_4, C_2H_6, and C_3H_8, CO_2 was strongly present, especially in the first stages of reaction, what negatively affected the heating value of the gaseous products. Finally, the formulated H_2 occurred during the dehydrogenation of aliphatic structures (Qing et al., 2022). These results demonstrate that big quantity of CH_4 recorded by gas online measurements was mixed with C_2H_6 and C_3H_8 gases. Also, these gases can be used for reception or separation using various advanced technologies, such as polymer membranes, in different separation conditions (Tonkonogovas et al., 2021; Mohamed et al., 2022).

The gaseous products synthesized from the pyrolyzed WMs samples at the end of all conversion process at 475, 500, 500, and 550 °C were analysed by GC–MS. Fig. 5 shows GC–MS analysis of the gaseous products formulated at the specified conditions. As shown, the spectroscopy shows several GC compounds with various peak areas, as listed in Table 3. As shown, 2,4-Dimethyl-1-heptene represented the major compound in all batches and its abundance increased with increasing pyrolysis temperature from 33.2% (475 °C) up to 38% (550 °C). Also, some quantities of Toluene were observed in 500 °C, 525 °C, and 550 °C batches in the range from 4.5 to 6.3%. The presence of these compounds in high abundance confirms that the synthesized gases were typical gaseous products in case of high heating values (Mumbach et al., 2019; Gupta et al., 2020). Finally, the chemical structure of the formulated gaseous products at 500 °C (optimum pyrolysis condition) was examined using FTIR and the spectroscopy is shown in Fig. 6A. The FTIR absorption showed a significant peak at 950 cm-1 due to C–O–C group and few FITR peaks with weak intensity at 1128 cm^{-1} (C–O–C group), 2970 cm^{-1} (C—H group), and 3353 cm^{-1} (hydroxyl group), hence manifesting a typical structure of biogas pyrolysis (Zakarauskas et al., 2021; Šereika et al., 2021).

3.3. GC analysis of liquid and wax products

In this section, the obtained tars and the condensable volatile products from each batch were analysed using GC/MS. Fig. 7 and Table 4 show GC/MS spectra of liquid/wax and the condensable volatile products obtained and their respective peak areas at 475, 500, 525, and 550 °C. It was observed that the tar fraction received from the pyrolysis of WMs samples at 475, 500, 525, and 550 °C had higher viscosity (wax product) when compared with 500 °C, which produced a fully liquid product (oil product). Based on GC/Ms. results, 2,4-Dimethyl-1-heptene (12.5–23.8%), 2-Undecene, 4-methyl- (4.7–7.3%), 2-Acetylcyclopentanone (4.75–14.5%), and 4-Isopropyl-1,3-cyclohexanedione (9–11.7%) were the main compounds in all the pyrolyzed WMs samples. These results confirm that the obtained pyrolysis tar products were typical oil and wax products rich in hydrocarbon molecules that can be used in various applications related to energy, lubrication, chemical industries, etc. (Jin et al., 2022; Missau et al., 2021; Hwang et al., 2021a, 2021b; Abdy et al., 2022a, 2022b; Wijesekara et al., 2021). As shown, the pyrolysis temperatures have a significant effect on the composition of the formulated pyrolysis tar products, where at 500 °C, the resulting tar was in liquid form because of complete decomposition of WMs always occurring at this temperature due to the full cracking reaction of carbohydrates of organic components in WMs into sugar molecules (Eimontas et al., 2021). Meanwhile, at lower temperature, the decomposition process did not have enough energy to break Van der Waals, hydrogen, β-1,4-glycosidic bonds of all WMs components (cellulose, lignin, and hemicellulose molecules) and formed several amorphous zones having small molecules joined together in form of viscous fluid (wax) (Lee et al., 2021a, 2021b, 2021c; Ali et al., 2022; Yousef et al., 2022; Li et al., 2022a, 2022b, 2022c). At higher pyrolysis temperatures (525 and 550 °C), the cracking reaction of oil increased and cracked their bonds breaking the molecules joined together and forming a viscous liquid again (wax) with higher yield and different composition when compared to 475 °C sample (Maqsood et al., 2021; Hwang et al., 2021a, 2021b). Finally, the obtained liquid fraction was examined using FTIR and the observed function groups are displayed in Fig. 6B. The FTIR spectra showed several functional groups at 3313 cm^{-1} (hydroxyl group), 2965 cm^{-1} (C—H group and aliphatic), 1378 cm^{-1} and 1455 cm^{-1} (N—O group), and 800–1100 cm^{-1} (C–O–C band and fingerprint region). These functional groups confirm that the synthesized fluid is an oil fuel (Zakarauskas et al., 2021).

3.4. Morphology and composition of the obtained chars

In the last phase of thermochemical reaction (devolatilization) of WMs, solid residues (SR) were formed in all samples in the form of very fine particles. The morphology and elemental analysis of these particles were observed using SEM and EDX analysis. Fig. 8A, B shows SEM images of char derived from WMs pyrolysis at 475 °C (lowest) and 550 °C (the highest temperature). As shown, the SR fraction in the tested samples contained very fine particles within micro-scale with a few bulk particles in the form of debris. Based on the EDX

Table 3
GC/MS Compounds of the gaseous products generated from the pyrolyzed WMs samples at different pyrolysis temperatures.

475 °C			500 °C			525 °C			550 °C		
Time (min.)	GC Compounds	Area (%)	Time (min.)	GC Compounds	Area (%)	Time (min.)	GC Compounds	Area (%)	Time (min.)	GC Compounds	Area (%)
3.425	2-Heptene, 4-methyl-, (*E*)-	1.63	2.49	1,3-Pentadiene, 2,3-dimethyl-	1.94	2.50	Cyclopentene, 4,4-dimethyl-	2.49	2.494	1,4-Hexadiene, 4-methyl-	2.55
3.620	Heptane, 4-methyl-	3.47	3.419	2-Heptene, 4-methyl-, (*E*)-	2.58	3.438	2-Heptene, 4-methyl-, (E)-	3.15	3.425	2-Heptene, 4-methyl-, (E)-	3.03
3.839	Cyclopentane, 1,2-dimethyl-3-methylene-, cis-	0.93	3.626	Toluene	4.48	3.645	Toluene	6.11	3.632	Toluene	6.26
4.409	1,2,4,4-Tetramethylcyclopentene	0.97	3.826	5,5-Dimethyl-1,3-hexadiene	2.47	3.839	Cyclohexene, 3-methyl-6-(1-methylethyl)-	3.31	3.826	5,5-Dimethyl-1,3-hexadiene	3.59
6.071	2,4-Dimethyl-1-heptene	31.17	4.952	3,4-Dimethyl cyclohexanone	1.16	4.428	Cyclopentene, 1,2,3-trimethyl-	1.38	4.952	1-Hexene, 3,3-dimethyl-	1.38
6.530	Cyclohexane, 1,3,5-trimethyl-, (1. alpha.,3.alpha.,5.beta.)-	0.94	6.045	2,4-Dimethyl-1-heptene	32.32	4.978	3,4-Dimethyl cyclohexanone	1.35	6.039	2,4-Dimethyl-1-heptene	37.91
7.171	1,2,4,4-Tetramethylcyclopentene	2.35	7.145	1,3-Heptadiene, 2,3-dimethyl-	4.32	6.064	2,4-Dimethyl-1-heptene	36.98	6.511	Cyclohexane, 1,3,5-trimethyl-	1.51
7.552	1,2,4,4-Tetramethylcyclopentene	1.86	7.533	6,6-Dimethylhepta-2,4-diene	1.91	6.543	Cyclohexane, 1,3,5-trimethyl-, (1. alpha.,3.alpha.,5.beta.)-	1.72	7.138	Cyclopropane, 1,1-dimethyl-2-(2-methyl-1-propenyl)-	5.16
8.193	Cyclopentane, 1,2,3,4,5-pentamethyl-	5.89	8.173	Cyclohexane, 1,1,3,5-tetramethyl-,cis-	5.46	7.164	p-Xylene	5.39	7.533	6,6-Dimethylhepta-2,4-diene	1.87
12.533	2-Decene, 4-methyl-, (*Z*)-	1.10	12.520	Cyclopentane, 1-butyl-2-ethyl-	1.95	7.559	6,6-Dimethylhepta-2,4-diene	2.33	8.167	2-Pentene, 4-methyl-, (*Z*)-	4.53
13.116	Nonane, 2,6-dimethyl-	1.27	15.936	Ethanone, 1-cyclopentyl-	4.65	8.199	Cyclohexane, 1,1,3,5-tetramethyl-,trans-	4.88	8.277	Bicyclo[3.1.1]heptan-2-one, 6,6-dimethyl-	1.18
13.284	Nonane, 2,6-dimethyl-	1.14	16.104	2-Undecene, 4-methyl-	3.48	8.303	Bicyclo[3.1.1]heptan-2-one, 6,6-dimethyl-	1.22	12.514	1,1,4-Trimethylcyclohexane	2.06
14.138	5-Undecene	1.12	18.69	2-Propen-1-one, 1-(2,2-dimethylcyclopropyl)-	1.23	12.533	2-Undecene, 4-methyl-	2.14	15.93	Cyclopentane, propyl-	4.65
15.955	2-Undecene, 4-methyl-	5.03	24.209	2-Acetylcyclopentanone	6.58	13.122	Nonane, 2,6-dimethyl-	1.26	16.097	Ethanone, 1-cyclopentyl-	3.28
16.117	2-Undecene, 4-methyl-	4.16	24.494	Cyclopentane, propyl-	2.76	13.283	Heptane, 3,3,5-trimethyl-	1.14	18.698	2-Propen-1-one, 1-(2,2-dimethylcyclopropyl)-	1.26
17.831	Cyclohexane, 1,1,3,5-tetramethyl-,trans-	0.98	24.765	4-Isopropyl-1,3-cyclohexanedione	5.22	15.949	1-Undecene, 7-methyl-	4.75	24.203	2-Acetylcyclopentanone	5.84
18.704	2-Propen-1-one, 1-(2,2-dimethylcyclopropyl)-	0.93	25.684	2,3-Dimethyl-3-heptene, (Z)-	1.15	16.117	Ethanone, 1-cyclopentyl-	3.76	24.487	Cyclopentane, propyl-	2.19
24.222	2-Acetylcyclopentanone	7.46	26.538	2-Propenoic acid, 2-methyl-, 3,3,5-trimethylcyclohexyl ester	1.35	24.215	2-Acetylcyclopentanone	5.39	24.765	4-Isopropyl-1,3-cyclohexanedione	4.51
24.500	Cyclooctane, 1-methyl-3-propyl-	4.00	31.072	Cyclohexane, 1-ethyl-2-propyl-	2.18	24.500	Cyclohexane, 1,2,3-trimethyl-, (1.	2.59	26.538	Cyclohexane, 2-propenyl-	1.15
24.778	4-Isopropyl-1,3-cyclohexanedione	6.38	31.881	Cyclohexane, 1,1,3,5-tetramethyl-,trans-	1.30	24.772	Cyclohexane, 1,2,4-trimethyl-	4.38	31.079	Cyclohexane, 1-ethyl-2-propyl-	1.52
25.691	2,3-Dimethyl-3-heptene, (*Z*)-	1.35	33.155	Cyclohexane, 1,1,3,5-tetramethyl-,trans-	1.59	31.079	Cyclohexane, 1-ethyl-2-propyl-	1.39	37.082	Bacchotricuneatin c	1.73
26.415	Cyclohexane, 1,1,3,5-tetramethyl-,cis-	1.07	37.082	Hexacosyl trifluoroacetate	2.60	37.088	Octacosyl trifluoroacetate	1.40	37.839	Nonadecyl pentafluoropropionate	1.56
26.538	2-Propenoic acid, 2-methyl-, 2-propenyl ester	1.07	37.845	Cyclohexane, 1-ethyl-2-propyl-	2.57	37.845	Cyclohexane, 1,2-diethyl-, cis-	1.52	38.977	p-Menthon-8-thiol	1.29
31.079	Cyclohexane, 1,2,4-trimethyl-	2.05	38.977	Cyclooctane, 1-methyl-3-propyl-	1.84						
31.364	1-Hexene, 3,3-dimethyl-	1.10	42.477	Triallylsilane	1.34						
31.88	Cyclohexane, 1,2,4-trimethyl-	1.62	44.22	1R,2c,3 t,4 *t*-Tetramethyl-cyclohexan	1.56						
33.155	Cyclopropanol, 1-(3,7-dimethyl-1-octenyl)-	1.24									
37.088	Hexacosyl trifluoroacetate	2.35									
37.845	Octacosyl trifluoroacetate	3.00									
38.712	Octacosyl trifluoroacetate	1.12									
38.971	Cyclohexane, 3-ethyl-5-methyl-1-propyl-	1.26									

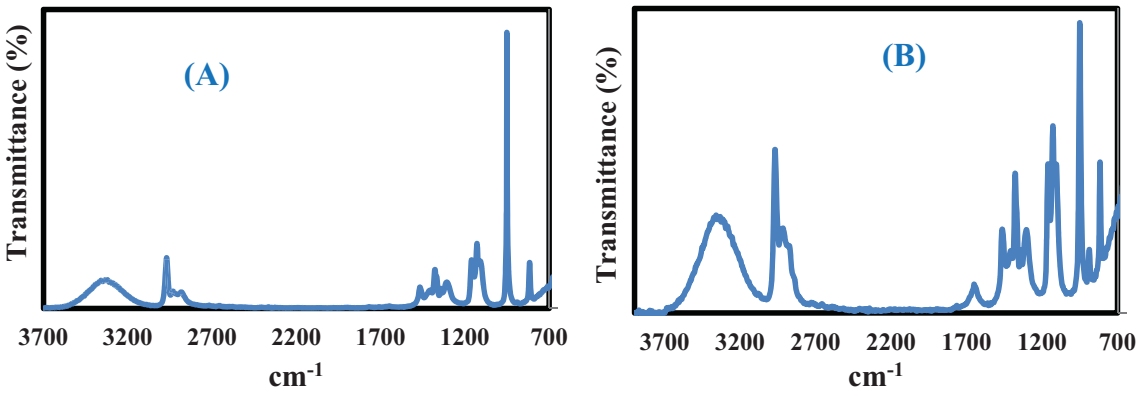

Fig. 6. FTIR of the obtained A) gaseous products and B) tars at 500 °C.

measurements, these particles were rich in calcium (Ca) (Fig. 8C, D). Also, the concentration of Ca was changing because of the treatment temperature in the range 41.95 to 45 wt%, as shown in Table 5. This element resulted from the middle layer of WMs, and could not decompose at such low decomposition temperatures, thus remaining in the char fraction (Harussani et al., 2022). Also, some heavy metals were noticed in the examined samples, such as Titanium, Magnesium, Zinc, etc. resulting from decomposition of pigments, which are composed of various elements (Yan et al., 2020). Based on this composition, the obtained char can be considered as a calcium-rich biochar that has many applications, for example, phosphorus removal, etc. (Li et al., 2022a, 2022b, 2022c). Also, the functional groups of the formulated char from each batch were determined using FTIR and the results are shown in Fig. 8E. The analysis showed that all samples were composed of three very similar functional groups: 2344 cm^{-1} due to O—H group, and 1428 and 877 cm^{-1} due to C—O and $CO^{2-}{}_3$ in Calcium carbonate ($CaCO_3$) (Li et al., 2022a, 2022b, 2022c; Zhang et al., 2020). The intensity $CaCO_3$ peak changed with increase in decomposition temperature and these results agree with EDX measurements.

3.5. Environmental impact assessment

In this part, the environmental impact of conversion of WMs into oil and wax products via pyrolysis was studied. All the calculated categories were based on the suggested layout (Fig. 2) and their impacts were compared to incineration process, as illustrated in Table 6 and Fig. 9A. Among all the calculated categories, the global warming (GW) item had the most important effect followed by terrestrial acidification (TA) factor, while the effect for Ozone formation, Human health (OFH), fine particulate matter formation (FP), ozone formation, Terrestrial ecosystems (OFT), terrestrial ecotoxicity (TE) and fossil resource scarcity (FR) was moderate. In case of the rest of other categories, almost no effect was noticed. Therefore, the discussion was focused on the most significant impacts (GW, OFH, FP, OFT, TE and ER) and their distribution, as shown in Fig. 9B. As indicated and regardless of the type of products obtained from pyrolysis processing, the treatment of WMs via pyrolysis showed a significant reduction in GW item compared to that managed using incineration with improvement in the range 90–94%. However, the pyrolysis process showed several additional environmental burdens represented by OFH, FP, OFT and TA items, which were nearly hidden in case of incineration practice. The effect of TE category was attended in both practices with almost similar score. Meanwhile, the pyrolysis treatment showed higher FR due to the energy consumed in starting the plant up and WMs decomposed thermally into oil and wax (Zakarauskas et al., 2021; Mohamed et al., 2021). Despite of this, pyrolysis treatment showed a total score much lower than incineration estimated at 56% for scenario A (oil) and 73% for scenario B (wax). This is due to higher heating value of wax (45 MJ/kg) compared to oil (24 MJ/kg) (https://pyrotechenergy.com; Abdy et al., 2022a, 2022b). Also, conversion of WMs into wax can reduce OFH, FP, OFT, and TA factors

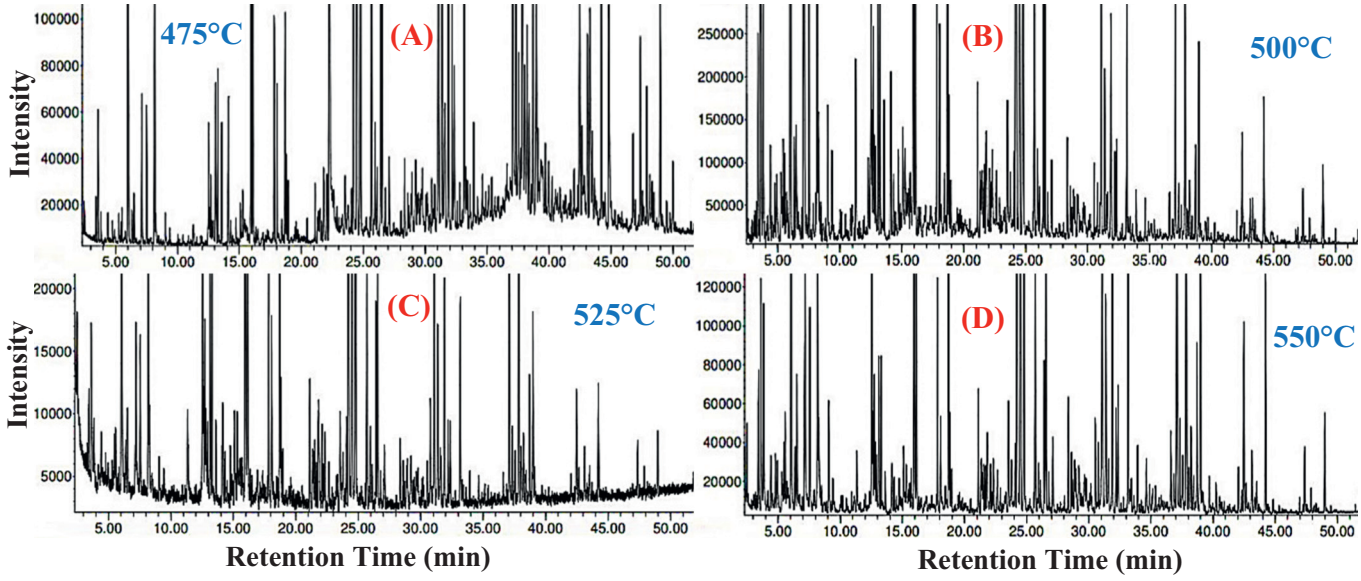

Fig. 7. GC/MS of tar products synthesized at A) 475 °C, B) 500 °C, C)525 °C and D) 550 °C.

Table 4
GC/MS Compounds of the tars generated from the pyrolyzed WMs samples at different pyrolysis temperatures.

475 °C			500 °C			525 °C			550 °C		
Time (min.)	GC Compounds	Area (%)	Time (min.)	GC Compounds	Area (%)	Time (min.)	GC Compounds	Area (%)	Time (min.)	GC Compounds	Area (%)
6.013	2,4-Dimethyl-1-heptene	12.51	3.619	Toluene	2.25	6.058	2,4-Dimethyl-1-heptene	14.21	3.645	Heptane, 4-methyl-	1.45
8.154	3-Octene, 2,2-dimethyl-	2.48	3.820	5,5-Dimethyl-1,3-hexadiene	1.18	7.197	2,4-Heptadiene, 2,6-dimethyl-	1.60	6.052	2,4-Dimethyl-1-heptene	23.77
15.923	2-Undecene, 4-methyl-	4.71	6.026	2,4-Dimethyl-1-heptene	23.62	8.199	1.alpha.,2.beta.,3.alpha.,4.beta.-Tetramethylcyclopentane	2.71	7.177	6,6-Dimethylhepta-2,4-diene	2.42
16.091	Cyclooctane, 1-methyl-3-propyl-	3.66	7.080	p-Xylene	1.60	12.540	1-Hexene, 3,3,5-trimethyl-	2.45	7.559	6,6-Dimethylhepta-2,4-diene	1.22
18.691	2-Propen-1-one, 1-(2,2-dimethylcyclopropyl)-	0.99	7.520	6,6-Dimethylhepta-2,4-diene	1.60	12.734	2-Decene, 4-methyl-, (*Z*)-	1.09	8.193	Cyclohexane, 1,1,3,5-tetramethyl-,trans-	3.24
24.203	2-Acetylcyclopentanone	13.89	8.154	Cyclohexane, 1,1,3,5-tetramethyl-,trans-	5.11	13.122	Heptane, 3,3,5-trimethyl-	1.71	12.533	Cyclopentane, 1-butyl-2-ethyl-	1.82
24.487	Cyclohexane, 1,2,4-trimethyl-	6.38	12.501	2-Decene, 4-methyl-, (*Z*)-	2.42	13.284	Octane, 2,3,6,7-tetramethyl-	1.55	15.949	2-Undecene, 4-methyl-	5.76
24.765	4-Isopropyl-1,3-cyclohexanedione	11.37	13.089	Nonane, 2,6-dimethyl-	1.37	15.949	Cyclooctane, 1-methyl-3-propyl-	8.80	16.117	Ethanone, 1-cyclopentyl-	4.02
25.677	2,3-Dimethyl-3-heptene, (*Z*)-	2.20	14.111	4-Octene, 2,6-dimethyl-, [S-(Z)]-	1.24	16.117	2-Undecene, 4-methyl-	6.99	17.831	Cyclohexane, 1,1,3,5-tetramethyl-,trans-	1.23
26.402	Cyclohexane, 1,1,3,5-tetramethyl-,cis-	1.75	15.929	2-Undecene, 4-methyl-	7.32	17.831	Dichloroacetic acid, 6-ethyl-3-octylester	1.85	18.711	2-Propen-1-one, 1-(2,2-dimethylcyclopropyl)-	1.96
26.531	2-Propenoic acid, 2-methyl-, 3,3,5-trimethylcyclohexyl ester	1.77	16.097	2-Undecene, 4-methyl-	5.51	18.070	2,5-Dihydro-5-methoxy-2-furanone	1.28	24.215	Cyclooctane, 1-methyl-3-propyl-	12.38
31.072	Cyclohexane, 1-ethyl-2-propyl-	3.40	17.812	Cyclohexane, 1,1,3,5-tetramethyl-,trans-	2.02	18.711	2-Propen-1-one, 1-(2,2-dimethylcyclopropyl)-	2.21	24.500	2-Acetylcyclopentanone	4.75
31.35	Cyclohexane, 1,1,3,5-tetramethyl-,trans-	1.85	18.69	2-Propen-1-one, 1-(2,2-dimethylcyclopropyl)-	2.47	21.835	1-Hexene, 3,3-dimethyl-	1.22	24.77	4-Isopropyl-1,3-cyclohexanedione	9.68
31.881	Cyclooctane, ethyl-	2.65	24.209	2-Acetylcyclopentanone	11.69	24.216	2-Acetylcyclopentanone	14.53	25.690	3-Decene, 2,2-dimethyl-, (E)-	1.58
32.185	Cyclohexane, 1,2,4-trimethyl-	1.03	24.487	Cyclohexane, 1,2,4-trimethyl-	4.94	24.494	Trichloroacetic acid, 6-ethyl-3-octylester	6.68	26.544	2-Propenoic acid, 2-methyl-, 3,3,5-trimethylcyclohexyl ester	2.83
33.14	Cyclohexane, 1,1,3,5-tetramethyl-,trans-	2.08	24.77	4-Isopropyl-1,3-cyclohexanedione	8.99	24.772	4-Isopropyl-1,3-cyclohexanedione	11.70	31.07	Nonadecyl pentafluoropropionate	3.72
37.082	Octacosyl trifluoroacetate	4.29	25.684	Cyclohexane, 1,1,3,5-tetramethyl-,cis-	2.12	25.690	Heptane, 2-methyl-3-methylene-	2.03	31.363	Cyclohexane, 1,2-diethyl-3-methyl-	1.27
37.327	Octacosyl trifluoroacetate	1.14	26.402	3-Decene, 2,2-dimethyl-, (*E*)-	1.39	26.415	Cyclohexane, 1,1,3,5-tetramethyl-,cis-	1.38	31.887	Heptafluorobutanoic acid, heptadecyl ester	2.04
37.838	Octacosyl trifluoroacetate	5.21	26.531	1,4-Hexadiene, 3,3,5-trimethyl-	2.42	26.544	Cyclohexane, 1,1′-(1,2-dimethyl-1,2-ethanediyl)bis-	2.10	33.162	Triallylsilane	2.95
38.052	Cyclohexane, 1,2,4-trimethyl-	1.08	31.072	Cyclohexane, 1-ethyl-2-propyl-	2.58	31.085	Cyclohexane, 1-ethyl-2-propyl-	2.76	37.088	Octacosyl trifluoroacetate	3.56
38.220	Triallylsilane	1.09	31.881	Cyclohexane, 1,2,4-trimethyl-	1.48	31.363	1-Trifluoroacetoxy-2-methylpentane	1.20	37.845	Octacosyl trifluoroacetate	3.12
38.705	Octacosyl trifluoroacetate	1.96	33.155	1,5-Heptadiene, 3,3-dimethyl-, (E)	1.78	31.887	1-Undecene, 8-methyl-	1.77	38.983	Bicyclo[3.1.1]heptan-3-one, 2,6,6-trimethyl-, (1.alpha.,2.beta.,5.alpha.)-	2.51
38.970	Bicyclo[3.1.1]heptan-3-one, 2,6,6-trimethyl-, (1.alpha.,2.beta.,5.alpha.)-	2.10	37.082	Tricosyl trifluoroacetate	1.88	33.162	8-Chloro-1-octanol, *tert*-butyldimethylsilylether	1.53	42.483	Tetracosyl heptafluorobutyrate	1.27
42.477	Hexacosyl heptafluorobutyrate	1.74	37.838	Octacosyl trifluoroacetate	1.77	37.088	Hexacosyl trifluoroacetate	2.46	44.229	Zinc, bis[2-(1,1-dimethylethyl)-3,3-dimethylcyclopropyl]-, [1.alpha. (1R*,2R*),2.beta.]-	1.44
43.104	Tricosyl trifluoroacetate	1.09	38.970	3,7-Nonadien-2-one, 4,8-dimethyl-	1.24	37.852	Tricosyl trifluoroacetate	2.98			
43.317	Fumaric acid, 3-fluorophenyl nonylester	1.64				38.984	Cyclohexane, 1,1,3,5-tetramethyl-,cis-	1.22			
44.223	Cyclohexane, 2,4-diethyl-1-methyl-	1.89									
44.850	4,4′-(Hexafluoroisopropylidene) diphenol	1.66									
47.373	Tetrapentacontane, 1,54-dibromo-	1.00									
48.977	Triallylsilane	1.38									

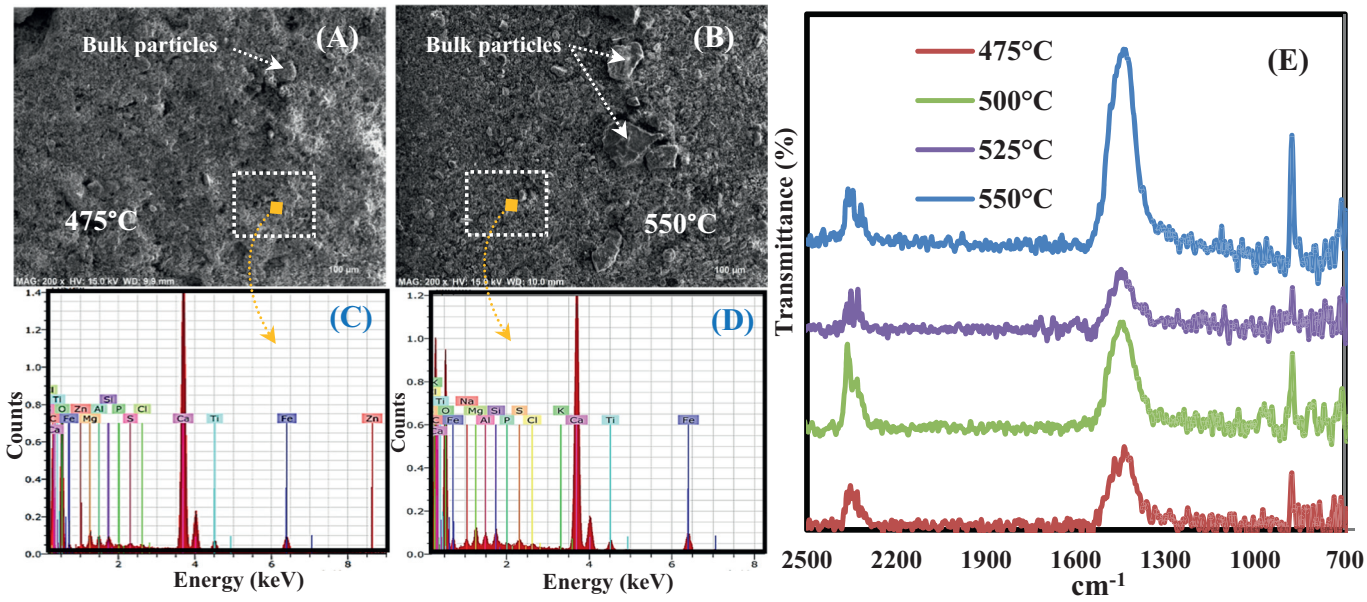

Fig. 8. A) SEM- EDX image of the formulated char product at A) 475 °C, B) 500 °C, C) 500 °C and D) 550 °C.

Table 5
EDX elemental analysis of the prepared char at different pyrolysis temperatures.

Sample	EDX elements														
	Carbon	Oxygen	Iron	Titanium	Calcium	Magnesium	Aluminum	Silicon	Sulfur	Chlorine	Zinc	Phosphorus	Sodium	Potassium	Copper
475 °C	8.03	38.56	7.30	2.13	39.34	1.16	0.70	0.66	0.38	0.41	1.13	0.21	–	–	–
500 °C	9.83	40.23	6.26	1.47	37.65	0.99	1.31	0.76	0.35	0.27		0.08	0.45	0.35	–
500 °C	14.33	40.12	5.74	4.77	27.62	1.38	0.69	0.49	0.71	0.11	2.10	0.02	0.25	0.02	1.65
550 °C	12.89	40.62	6.72	2.14	33.89	1.02	0.53	0.65	0.42	0.25		0.11	0.60	0.15	–

by approximately 38% compared to the oil scenario, hence, contributing to bigger benefit to human and ecosystem's health. Based on the estimated LCA, conversion of WMs into oil and wax products via pyrolysis has a great potential to be applied at the industrial scale with high environmental impact, especially on global warming, and only few onsite emissions of particular matter should be taken into consideration when designing the treatment plant. Also, these results demonstrate that treating WMs as a mixture has a significant effect on the formulated pyrolysis products (oil or wax) and their LCA compared to considering each layer of WMs individually, when only oil is generated (Li et al., 2022a, 2022b, 2022c).

3.6. Economic performance

The economic performance of the proposed thermal conversion process for processing one kg of WMs was determined in this section based on the electricity input for pre-treatment and pyrolysis (0.136 kWh/kg × 0.12 $/kWh) and the output products. The electric power

Table 6
Environmental impacts of transforming WMs into oil and wax compared to incineration approach.

Impact category		Unit	Pyrolysis treatment		Polypropylene incineration
			Scenario A (500 °C) Oil	Scenario B (525 °C) Wax	
A	Global warming (GW)	kg CO_2 eq	0.244416136	0.151120708	2.537848627
B	Stratospheric ozone depletion	kg CFC11 eq	6.91381×10^{-09}	4.27476×10^{-09}	5.90966×10^{-08}
C	Ionizing radiation	kBq Co-60 eq	8.54986×10^{-05}	5.28632×10^{-05}	4.57327×10^{-06}
D	Ozone formation, Human health (OFH)	kg NO_x eq	0.080066983	0.04950483	0.000392018
E	Fine particulate matter formation (FP)	kg PM2.5 eq	0.096297144	0.059539819	7.09783×10^{-05}
F	Ozone formation, Terrestrial ecosystems (OFT)	kg NO_x eq	0.128707305	0.079578785	0.000400254
G	Terrestrial acidification (TA)	kg SO_2 eq	0.331958834	0.205247718	0.000183135
H	Freshwater eutrophication	kg P eq	4.76395×10^{-06}	2.94552×10^{-06}	9.09177×10^{-07}
I	Marine eutrophication	kg N eq	9.42178×10^{-07}	5.82542×10^{-07}	9.60795×10^{-07}
J	Terrestrial ecotoxicity (TE)	kg 1,4-DCB	0.098632004	0.060983447	0.070591946
K	Freshwater ecotoxicity	kg 1,4-DCB	3.44265×10^{-05}	2.12856×10^{-05}	0.000284649
L	Marine ecotoxicity	kg 1,4-DCB	9.55081×10^{-05}	5.90519×10^{-05}	0.000456108
M	Human carcinogenic toxicity	kg 1,4-DCB	0.000984503	0.000608711	0.003458502
N	Human non-carcinogenic toxicity	kg 1,4-DCB	0.00192749	0.001191753	0.002812515
O	Land use	m2a crop eq	0.000567611	0.00035095	0.000835043
P	Mineral resource scarcity	kg Cu eq	4.66174×10^{-05}	2.88232×10^{-05}	0.000203592
Q	Fossil resource scarcity (FR)	kg oil eq	0.157234008	0.097216636	0.004364263
R	Water consumption	m^3	0.001594964	0.000986154	0.000544909
Total score			1.142654745	0.706495068	2.622453041

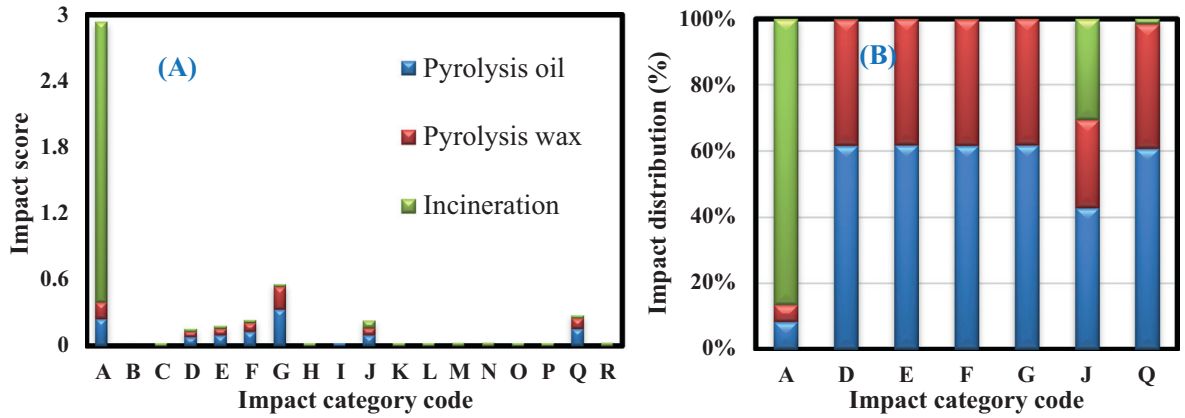

Fig. 9. Environmental impacts of pyrolysis of WMs compared to incineration treatment.

calculation was made based on the pyrolysis cycle (200 g), then the calculation was promoted to 1 kg, only to display the data per kg of WMs. Regarding the output items, the economic analysis for both scenarios (A and B) was calculated, and all the items and their trade prices are included in Table 7. As shown, the oil production scenario has a significant contribution to the economic sector with an 85% improvement compared to the wax production scenario. The cost of treating air emissions has been neglected because there is currently an advanced technology that can be used to capture these adsorbed gases such as the membrane technology. This separation technique is characterized by its low cost, system compactness, less energy, simplicity, and ability to use them for long time (Yong et al., 2022).

4. Conclusions

In the present research, the pyrolysis of surgical mask waste (WMs) as a mixture was studied using an experimental set-up with capacity of 200 g at 475, 500, 525, and 550 °C. The results showed that the maximum yield of pyrolysis oil can be obtained at 500 °C (42.3%), while the maximum yield of wax product was achieved at 525 °C (36.4%). Whereas the gaseous products obtained were rich in methane, ethane, and propane, which helps in increasing their heating value, especially at the highest pyrolysis temperature. Besides, the environmental performance of the proposed treatment was examined in the form of different categories using life cycle analysis. The environmental assessment showed that the proposed pyrolysis treatment has a lower overall environmental impact, especially on global warming combined with a smaller score compared to management of WMs using incineration treatment with a significant improvement estimated at 56% (in case of the oil production scenario) and 73% (in case of the wax production scenario). Based on the reported results, pyrolysis treatment at 525 °C is highly recommended to convert WMs into wax product with high environmental performance and moderate economic performance.

Table 7
Commercial prices for input and output items for both scenarios.

	Item	Commercial price (Zakarauskas et al., 2021; Mohamed et al., 2021)	Cost of scenario (A)	Cost of scenario (B)
Input	Electric power	0.12 $/kWh	0.136 $/kg	
Outputs	Oil	8.4 $/kg	3.550	–
	Wax	0.9 $/kg	–	0.328
	gas	0.6 $/kg	0.325	0.356
	Char	0.002	0.002	0.003
The total profitability			3.741	0.551

Declaration of competing interest

The authors declare that they have no known competing financial interests or personal relationships that could have appeared to influence the work reported in this paper.

Acknowledgment

This project has received funding from European Regional Development Fund (project No 13.1.1-LMT-K-718-05-0017) under grant agreement with the Research Council of Lithuania (LMTLT). Funded as European Union's measure in response to Cov-19 pandemic.

References

Abdelnaby, M.A., Eimontas, J., Striūgas, N., 2021. Pyrolysis and gasification kinetic behavior of mango seed shells using TG-FTIR-GC–MS system under N2 and CO2 atmospheres. Renew. Energy https://doi.org/10.1016/j.renene.2021.04.034.

Abdy, C., Zhang, Y., Wang, J., Yang, Y., Artamendi, I., Allen, B., 2022. Pyrolysis of polyolefin plastic waste and potential applications in asphalt road construction: a technical review. Resour. Conserv. Recycl. https://doi.org/10.1016/j.resconrec.2022.106213.

Abdy, C., Zhang, Y., Wang, J., Yang, Y., Artamendi, I., Allen, B., 2022. Pyrolysis of polyolefin plastic waste and potential applications in asphalt road construction: a technical review. Resour. Conserv. Recycl. https://doi.org/10.1016/j.resconrec.2022.106213.

Ali, L., Kuttiyathil, M.S., Altarawneh, M., 2022. Catalytic upgrading of the polymeric constituents in Covid-19 masks. J. Environ. Chem. Eng. https://doi.org/10.1016/j.jece.2021.106978.

Amuah, E.E.Y., Agyemang, E.P., Dankwa, P., Fei-Baffoe, B., Kazapoe, R.W., Douti, N.B., 2022. Are used face masks handled as infectious waste? Novel pollution driven by the COVID-19 pandemic. Resour. Conserv. Recycl. Adv. https://doi.org/10.1016/j.rcradv.2021.200062.

Ardila-Suárez, C., Pablo Villegas, J., de Barros, Lins, Neto, E., Ghislain, T., Lavoie, J.M., 2022. Waste surgical masks to fuels via thermochemical co-processing with waste motor oil and biomass. Bioresour. Technol. https://doi.org/10.1016/j.biortech.2022.126798.

Brillard, A., Kehrli, D., Douguet, O., Gautier, K., Tschamber, V., Bueno, M.A., Brilhac, J.F., 2021. Pyrolysis and combustion of community masks: thermogravimetric analyses, characterizations, gaseous emissions, and kinetic modeling. Fuel https://doi.org/10.1016/j.fuel.2021.121644.

Das, Sonali, Sarkar, S., Das, A., Das, Shreyosree, Chakraborty, P., Sarkar, J., 2021. A comprehensive review of various categories of face masks resistant to Covid-19. Clin. Epidemiol. Glob. Health https://doi.org/10.1016/j.cegh.2021.100835.

Dastjerdi, B., Strezov, V., Rajaeifar, M.A., Kumar, R., Behnia, M., 2021. A systematic review on life cycle assessment of different waste to energy valorization technologies. J. Clean. Prod. https://doi.org/10.1016/j.jclepro.2020.125747.

Dharmaraj, S., Ashokkumar, V., Pandiyan, R., Halimatul Munawaroh, H.S., Chew, K.W., Chen, W.H., Ngamcharussrivichai, C., 2021. Pyrolysis: an effective technique for degradation of COVID-19 medical wastes. Chemosphere https://doi.org/10.1016/j.chemosphere.2021.130092.

Eimontas, J., Striūgas, N., Abdelnaby, M.A., 2021a. Pyrolysis kinetic behaviour and TG-FTIR-GC–MS analysis of coronavirus face masks. J. Anal. Appl. Pyrolysis https://doi.org/10.1016/j.jaap.2021.105118.

Eimontas, J., Striūgas, N., Abdelnaby, M.A., Yousef, S., 2021b. Catalytic pyrolysis kinetic behavior and TG-FTIR-GC–MS analysis of metallized food packaging plastics with different concentrations of ZSM-5 zeolite catalyst. Polymers https://doi.org/10.3390/polym13050702.

Farooq, A., Lee, J., Song, H., Ko, C.H., Lee, I.H., Kim, Y.M., Rhee, G.H., Pyo, S., Park, Y.K., 2022. Valorization of hazardous COVID-19 mask waste while minimizing hazardous

byproducts using catalytic gasification. J. Hazard. Mater. https://doi.org/10.1016/j.jhazmat.2021.127222.
Forouzandeh, P., O'Dowd, K., Pillai, S.C., 2021. Face masks and respirators in the fight against the COVID-19 pandemic: an overview of the standards and testing methods. Saf. Sci. https://doi.org/10.1016/j.ssci.2020.104995.
Gala, A., Guerrero, M., Serra, J.M., 2020. Characterization of post-consumer plastic film waste from mixed MSW in Spain: a key point for the successful implementation of sustainable plastic waste management strategies. Waste Manag. https://doi.org/10.1016/j.wasman.2020.05.019.
Gupta, A., Thengane, S.K., Mahajani, S., 2020. Kinetics of pyrolysis and gasification of cotton stalk in the central parts of India. Fuel https://doi.org/10.1016/j.fuel.2019.116752.
Harussani, M.M., Sapuan, S.M., Rashid, U., Khalina, A., Ilyas, R.A., 2022. Pyrolysis of polypropylene plastic waste into carbonaceous char: priority of plastic waste management amidst COVID-19 pandemic. Sci. Total Environ. https://doi.org/10.1016/j.scitotenv.2021.149911.
https://blog.gotopac.com/2020/05/07/why-3-ply-face-masks-and-surgical-masks-are-meaningful-n95-mask-alternatives/, n.d.https://blog.gotopac.com/2020/05/07/why-3-ply-face-masks-and-surgical-masks-are-meaningful-n95-mask-alternatives/
https://pyrotechenergy.com/, n.d.https://pyrotechenergy.com/
https://www.fda.gov/medical-devices/personal-protective-equipment-infection-control/n95-respirators-surgical-masks-and-face-masks, n.d.https://www.fda.gov/medical-devices/personal-protective-equipment-infection-control/n95-respirators-surgical-masks-and-face-masks
Hwang, K.R., Choi, S.A., Choi, I.H., Lee, K.H., 2021. Catalytic cracking of chlorinated heavy wax from pyrolysis of plastic wastes to low carbon-range fuels: catalyst effect on properties of liquid products and dechlorination. J. Anal. Appl. Pyrolysis https://doi.org/10.1016/j.jaap.2021.105090.
Hwang, K.R., Choi, S.A., Choi, I.H., Lee, K.H., 2021. Catalytic cracking of chlorinated heavy wax from pyrolysis of plastic wastes to low carbon-range fuels: catalyst effect on properties of liquid products and dechlorination. J. Anal. Appl. Pyrolysis https://doi.org/10.1016/j.jaap.2021.105090.
Jin, X., Lee, J.H., Choi, J.W., 2022. Catalytic co-pyrolysis of woody biomass with waste plastics: effects of HZSM-5 and pyrolysis temperature on producing high-value pyrolytic products and reducing wax formation. Energy https://doi.org/10.1016/j.energy.2021.121739.
Jung, S., Lee, S., Dou, X., Kwon, E.E., 2021. Valorization of disposable COVID-19 mask through the thermo-chemical process. Chem. Eng. J. https://doi.org/10.1016/j.cej.2020.126658.
Kang, A., Ren, L., Hua, C., Song, H., Dong, M., Fang, Z., Zhu, M., 2021. Environmental management strategy in response to COVID-19 in China: based on text mining of government open information. Sci. Total Environ. https://doi.org/10.1016/j.scitotenv.2021.145158.
Khoo, H.H., 2019. LCA of plastic waste recovery into recycled materials, energy and fuels in Singapore. Resour. Conserv. Recycl. https://doi.org/10.1016/j.resconrec.2019.02.010.
Kliucininkas, L., Eimontas, J., Striūgas, N., Tatariants, M., Abdelnaby, M.A., Tuckute, S., 2019. A sustainable bioenergy conversion strategy for textile waste with self-catalysts using mini-pyrolysis plant. Energy Convers. Manag. https://doi.org/10.1016/j.enconman.2019.06.050.
Kliucininkas, L., Tatariants, M., Tichonovas, M., Sarwar, Z., Jonuškienė, I., 2019. A new strategy for using textile waste as a sustainable source of recovered cotton. Resour. Conserv. Recycl. https://doi.org/10.1016/j.resconrec.2019.02.031.
Kuliešienė, N., Sakalauskaitė, S., Nenartavičius, T., Daugelavičius, R., 2021. Sustainable green strategy for recovery of glucose from end-of-life euro banknotes. Waste Manag. https://doi.org/10.1016/j.wasman.2021.01.007.
Lan, D.Y., Zhang, H., Wu, T.W., Lü, F., Shao, L.M., He, P.J., 2022. Repercussions of clinical waste co-incineration in municipal solid waste incinerator during COVID-19 pandemic. J. Hazard. Mater. https://doi.org/10.1016/j.jhazmat.2021.127144.
Lee, A.W.L., Neo, E.R.K., Khoo, Z.Y., Yeo, Z., Tan, Y.S., Chng, S., Yan, W., Lok, B.K., Low, J.S.C., 2021. Life cycle assessment of single-use surgical and embedded filtration layer (EFL) reusable face mask. Resour. Conserv. Recycl. https://doi.org/10.1016/j.resconrec.2021.105580.
Lee, S.B., Lee, J., Tsang, Y.F., Kim, Y.M., Jae, J., Jung, S.C., Park, Y.K., 2021. Production of value-added aromatics from wasted COVID-19 mask via catalytic pyrolysis. Environ. Pollut. https://doi.org/10.1016/j.envpol.2021.117060.
Lee, S.B., Lee, J., Tsang, Y.F., Kim, Y.M., Jae, J., Jung, S.C., Park, Y.K., 2021. Production of value-added aromatics from wasted COVID-19 mask via catalytic pyrolysis. Environ. Pollut. https://doi.org/10.1016/j.envpol.2021.117060.
Li, C., Sun, Y., Yi, Z., Zhang, L., Zhang, S., Hu, X., 2022. Co-pyrolysis of coke bottle wastes with cellulose, lignin and sawdust: impacts of the mixed feedstock on char properties. Renew. Energy https://doi.org/10.1016/j.renene.2021.09.103.
Li, C., Yuan, X., Sun, Z., Suvarna, M., Hu, X., Wang, X., Ok, Y.S., 2022. Pyrolysis of waste surgical masks into liquid fuel and its life-cycle assessment. Bioresour. Technol. https://doi.org/10.1016/j.biortech.2021.126582.
Li, S., Li, J., Chen, H., Xu, J., 2022. Understanding the release behavior of biomass model components and coal in the co-pyrolysis process. J. Energy Inst. https://doi.org/10.1016/j.joei.2022.01.003.
Liang, H., Ji, Y., Ge, W., Wu, J., Song, N., Yin, Z., Chai, C., 2022. Release kinetics of microplastics from disposable face masks into the aqueous environment. Sci. Total Environ. https://doi.org/10.1016/j.scitotenv.2021.151650.
Maqsood, T., Dai, J., Zhang, Y., Guang, M., Li, B., 2021. Pyrolysis of plastic species: a review of resources and products. J. Anal. Appl. Pyrolysis https://doi.org/10.1016/j.jaap.2021.105295.
Mayanti, B., Helo, P., 2022. Closed-loop supply chain potential of agricultural plastic waste: economic and environmental assessment of bale wrap waste recycling in Finland. Int. J. Prod. Econ. https://doi.org/10.1016/j.ijpe.2021.108347.
Missau, J., Bertuol, D.A., Tanabe, E.H., 2021. Development of a nanostructured filter for pyrolysis wax purification: effects of particulate filter aids. Particuology https://doi.org/10.1016/j.partic.2020.02.005.
Mohamed, A., Eimontas, J., Zakarauskas, K., Striūgas, N., 2021. A new strategy for using lint-microfibers generated from clothes dryer as a sustainable source of renewable energy. Sci. Total Environ. https://doi.org/10.1016/j.scitotenv.2020.143107.
Mohamed, A., Yousef, S., Tonkonogovas, A., Makarevicius, V., Stankevičius, A., 2022. High performance of PES-GNs MMMs for gas separation and selectivity. Arab. J. Chem. https://doi.org/10.1016/j.arabjc.2021.103565.
Mumbach, G.D., Alves, J.L.F., Da Silva, J.C.G., De Sena, R.F., Marangoni, C., Machado, R.A.F., Bolzan, A., 2019. Thermal investigation of plastic solid waste pyrolysis via the deconvolution technique using the asymmetric double sigmoidal function: determination of the kinetic triplet, thermodynamic parameters, thermal lifetime and pyrolytic oil composition for clean energy recovery. Energy Convers. Manag. https://doi.org/10.1016/j.enconman.2019.112031.
Mumladze, T., Yousef, S., Tatariants, M., Kriukiene, R., Makarevicius, V., Lukošiute, S.I., Bendikiene, R., Denafas, G., 2018. Sustainable approach to recycling of multilayer flexible packaging using switchable hydrophilicity solvents. Green Chem. https://doi.org/10.1039/c8gc01062e.
Naimi, L.J., Sokhansanj, S., 2018. Data-based equation to predict power and energy input for grinding wheat straw, corn stover, switchgrass, miscanthus, and canola straw. Fuel Process. Technol. https://doi.org/10.1016/j.fuproc.2017.12.024.
Papari, S., Bamdad, H., Berruti, F., 2021. Pyrolytic conversion of plastic waste to value-added products and fuels: a review. Materials https://doi.org/10.3390/ma14102586.
Praspaliauskas, M., Eimontas, J., Striūgas, N., Zakarauskas, K., Abdelnaby, M.A., 2020. Pyrolysis kinetic behavior and TG-FTIR-GC–MS analysis of metallised food packaging plastics. Fuel https://doi.org/10.1016/j.fuel.2020.118737.
Purnomo, C.W., Kurniawan, W., Aziz, M., 2021. Technological review on thermochemical conversion of COVID-19-related medical wastes. Resour. Conserv. Recycl. https://doi.org/10.1016/j.resconrec.2021.105429.
Qing, W., Xinmin, W., Shuo, P., 2022. Study on the structure, pyrolysis kinetics, gas release, reaction mechanism, and pathways of Fushun oil shale and kerogen in China. Fuel Process. Technol. https://doi.org/10.1016/j.fuproc.2021.107058.
Ray, S.S., Lee, H.K., Huyen, D.T.T., Chen, S.S., Kwon, Y.N., 2022. Microplastics waste in environment: a perspective on recycling issues from PPE kits and face masks during the COVID-19 pandemic. Environ. Technol. Innov. https://doi.org/10.1016/j.eti.2022.102290.
Sangkham, S., 2020. Face mask and medical waste disposal during the novel COVID-19 pandemic in Asia. Case Stud. Chem. Environ. Eng. https://doi.org/10.1016/j.cscee.2020.100052.
Santos, J., Pizzol, M., Azarijafari, H., 2022. Life cycle assessment (LCA) of using recycled plastic waste in road pavements: theoretical modeling. Plastic Waste for Sustainable Asphalt Roads https://doi.org/10.1016/b978-0-323-85789-5.00014-9.
Šereika, J., Tonkonogovas, A., Hashem, T., Mohamed, A., 2021. CO2/CH4, CO2/N2 and CO2/H2 selectivity performance of PES membranes under high pressure and temperature for biogas upgrading systems. Environ. Technol. Innov. https://doi.org/10.1016/j.eti.2020.101339.
Shammi, M., Rahman, M.M., Ali, M.L., Khan, A.S.M., Siddique, M.A.B., Ashadudzaman, M., Bodrud-Doza, M., Alam, G.M.M., Tareq, S.M., 2022. Application of short and rapid strategic environmental assessment (SEA) for biomedical waste management in Bangladesh. Case Stud. Chem. Environ. Eng. https://doi.org/10.1016/j.cscee.2021.100177.
Striūgas, N., Eimontas, J., Praspaliauskas, M., Abdelnaby, M.A., 2021. Pyrolysis kinetic behaviour of glass fibre-reinforced epoxy resin composites using linear and nonlinear isoconversional methods. Polymers https://doi.org/10.3390/polym13101543.
Sun, S., Yuan, Y., Chen, R., Xu, X., Zhang, D., 2021. Kinetic, thermodynamic and chemical reaction analyses of typical surgical face mask waste pyrolysis. Therm. Sci. Eng. Prog. https://doi.org/10.1016/j.tsep.2021.101135.
Tcharkhtchi, A., Abbasnezhad, N., Zarbini Seydani, M., Zirak, N., Farzaneh, S., Shirinbayan, M., 2021. An overview of filtration efficiency through the masks: mechanisms of the aerosols penetration. Bioact. Mater. https://doi.org/10.1016/j.bioactmat.2020.08.002.
Tonkonogovas, A., Tuckute, S., Stankevičius, A., Mohamed, A., 2021. Ultra-permeable CNTs/PES membranes with a very low CNTs content and high H2/N2 and CH4/N2 selectivity for clean energy extraction applications. J. Mater. Res. Technol. https://doi.org/10.1016/j.jmrt.2021.10.125.
Torres, F.G., De-la-Torre, G.E., 2021. Face mask waste generation and management during the COVID-19 pandemic: an overview and the Peruvian case. Sci. Total Environ. https://doi.org/10.1016/j.scitotenv.2021.147628.
Trofimov, E., Eimontas, J., Striūgas, N., Hamdy, M., Abdelnaby, M.A., 2020. Conversion of end-of-life cotton banknotes into liquid fuel using mini-pyrolysis plant. J. Clean. Prod. https://doi.org/10.1016/j.jclepro.2020.121612.
Wijesekara, D.A., Sargent, P., Ennis, C.J., Hughes, D., 2021. Prospects of using chars derived from mixed post waste plastic pyrolysis in civil engineering applications. J. Clean. Prod. https://doi.org/10.1016/j.jclepro.2021.128212.
Xu, D., Lin, J., Ma, R., Fang, L., Sun, S., Luo, J., 2022. Microwave pyrolysis of biomass for low-oxygen bio-oil: mechanisms of CO2-assisted in-situ deoxygenation. Renew. Energy https://doi.org/10.1016/j.renene.2021.11.069.
Yan, L., Tatariants, M., Tichonovas, M., Kliucininkas, L., Lukošiūtė, S.I., 2020. Sustainable green technology for recovery of cotton fibers and polyester from textile waste. J. Clean. Prod. https://doi.org/10.1016/j.jclepro.2020.120078.
Yeo, Yong Ho, Gawk, Min A., Lee, Su Yeon, Nam, Young Sik, Park, Won Ho, 2022. Air purifier using super-absorbent polymer for removing air contaminants. Environ. Chem. Eng. https://doi.org/10.1016/j.jece.2022.107832.
Yousef, S., Eimontas, J., Striūgas, N., Mohamed, A., Abdelnaby, M.A., 2021. Morphology, compositions, thermal behavior and kinetics of pyrolysis of lint-microfibers

generated from clothes dryer. J. Anal. Appl. Pyrolysis https://doi.org/10.1016/j.jaap.2021.105037.

Yousef, S., Eimontas, J., Striūgas, N., Abdelnaby, M.A., 2022. A new strategy for butanol extraction from COVID-19 mask using catalytic pyrolysis process over ZSM-5 zeolite catalyst and its kinetic behavior. Thermochim. Acta https://doi.org/10.1016/j.tca.2022.179198.

Yu, R., Wen, X., Liu, J., Wang, Y., Chen, X., Wenelska, K., Mijowska, E., Tang, T., 2021. A green and high-yield route to recycle waste masks into CNTs/Ni hybrids via catalytic carbonization and their application for superior microwave absorption. Appl. Catal. B Environ. https://doi.org/10.1016/j.apcatb.2021.120544.

Zakarauskas, K., Eimontas, J., Striūgas, N., 2021. Microcrystalline paraffin wax, biogas, carbon particles and aluminum recovery from metallised food packaging plastics using pyrolysis, mechanical and chemical treatments. J. Clean. Prod. https://doi.org/10.1016/j.jclepro.2021.125878.

Zhang, C., Zhang, Z., Zhang, L., Li, Q., Li, C., Chen, G., Zhang, S., Liu, Q., Hu, X., 2020. Evolution of the functionalities and structures of biochar in pyrolysis of poplar in a wide temperature range. Bioresour. Technol. https://doi.org/10.1016/j.biortech.2020.123002.